ELSEVIER

Journal of Neuroscience Methods 78 (1997) 115–123

JOURNAL OF NEUROSCIENCE METHODS

A method for functional magnetic resonance imaging of olfaction

N. Sobel [a,*], V. Prabhakaran [a], J.E. Desmond [b], G.H. Glover [c], E.V. Sullivan [a,d], J.D.E. Gabrieli [a,b]

[a] *Department of Neuroscience, Stanford University, Jordan Hall, Building 420, Stanford, CA 94305, USA*
[b] *Department of Psychology, Stanford University, Stanford, CA 94305, USA*
[c] *Department of Radiology, Stanford University, Stanford, CA 94305, USA*
[d] *Department of Psychiatry and Behavioral Sciences, Stanford University, Stanford, CA 94305, USA*

Received 29 January 1997; received in revised form 20 June 1997; accepted 14 August 1997

Abstract

A method for generating olfactory stimuli for humans within a functional magnetic resonance imaging (fMRI) experimental design is described. The system incorporates a nasal-mask in which the change from odorant to no-odorant conditions occurs in less than 500 ms and is not accompanied by visual, auditory, tactile, or thermal cues. The mask provides an ordorant-free environment following prolonged ordorant presence. Specific imaging parameters that are conducive to the study of the human olfactory system are described. In a pilot study performed using these methods, the specific patterns of activation observed converged with published experimental and clinical findings. © 1997 Elsevier Science B.V.

Keywords: Olfaction; Trigeminal; Olfactometer; Human brain imaging; Functional magnetic resonance imaging; fMRI; Odor perception

1. Introduction

Functional magnetic resonance imaging (fMRI) offers a means of revealing neural substrates of olfactory functions, such as odor detection, recognition and identification. Applying fMRI to the study of olfaction necessitates development of odor-stimuli generation methods that not only adhere to the general guidelines of olfactory research, but also comply with specific limitations posed by the magnetic environment. Existing methods of air-dilution olfactometry were designed primarily for use in behavioral and electrophysiology studies (for reviews see: Kobal, 1985; Kobal and Hummel, 1991; Doty and Kobal, 1995; Prah et al., 1995). Olfactometry was also adopted to the magnetoencephalographic (MEG) environment (Kettenmann et al., 1996) and has recently been introduced to the fMRI environment by our and other groups (Sobel et al., 1996, 1997a; Kettenmann et al., 1997; Yousem et al., 1997).

When applying olfactometry to the fMRI environment, one must take in to account the limitations posed by the strong magnetic field that prevents the introduction of ferrous materials in the vicinity of the magnet bore. In addition, in contrast to the short duration stimulations sought in electrophysiological studies (on the order of 200 ms), block-design fMRI studies call for relatively long periods of stimulation (on the order of tens of seconds). Thus, the odor-stimuli generating apparatus must offer a way of rapidly clearing the odor that has accumulated around the subject during the extended period of stimulation (for other methods of fMRI analysis, such as single trial analysis, short duration stimuli may be preferable). Finally, an odor stimulus-generating apparatus fit for the fMRI environment must enable the experimenter, who is at a distance from the subject, to synchronously present instructions, col-

* Corresponding author. Tel.: +1 415 7250797; fax: +1 415 7255699; e-mail: nsobel@leland/stanford.edu

PII S0165-0270(97)00140-4

lect responses and control stimuli, without adding sources of stimulation variance.

The design of functional imaging studies typically involves comparing two conditions (e.g. Posner et al., 1988; Desmond et al., 1995; Gabrieli et al., 1996). Ideally, the difference between these conditions is limited to the process of interest alone. In an imaging study of olfaction, one condition may involve odorant presentation (odor phase) and the other condition may be identical but without any odorant presented (no-odor phase). In order to maintain the integrity of both the odor and no-odor phases, the experimental design must adhere to the following general guidelines of olfactory experimentation:

1.1. Purity

The no-odor phase should consist of pure-air, uncontaminated by odor molecules. The odor phase should consist of a known odorant at a known concentration.

1.2. Thermal regulation

Because different odors may have different carrier-base temperature, both the odorized and non-odorized air should be at the same temperature and humidity level, to avoid imaging a thermal, rather than an olfactory, response.

1.3. Tactile regulation

Tactile stimulation due to the stimulus generation ought to be held constant over the odor and no-odor phases in order to avoid imaging a tactile, rather than an olfactory, response.

Furthermore, brain-activation experiments require accurate temporal control over the stimulus (i.e. odor rise and fall times), because the acquisition of data must be linked to specific time-courses of stimulation. Therefore, the odor rise and fall time in an olfactometer designed for fMRI should be shorter than the rise time of the fMRI signal (blood oxygen-level dependency) which is in the range of several seconds (Bandettini et al., 1992).

In previous imaging studies of human olfaction using positron emission tomography (PET) (Zatorre et al., 1992) and fMRI (Koizuka et al., 1994), odor stimuli were generated by instructing the subject to inhale during presentation of a cotton wand that was either odorless or bearing an odor, or by inhaling from bags containing the odorant (Zald and Pardo, 1997). These means of odor presentation do not preclude the above mentioned sources of possible no-odor phase contamination, nor do they permit optimal control over temporal resolution or odor concentration. We describe a method generating olfactory stimuli that meets the above criteria and is suitable for a variety of olfactory experiments within an fMRI design.

2. Methods

2.1. Odor generation

The stimulus generator (Fig. 1) consists of two pumps, a main pump and a dilution pump, both situated in a room adjacent to the magnet room. Air from the main pump (non-lubricated by Gast, Bridgman, MI) is passed through an activated charcoal filter at 3.52 kg/cm^2 (50 PSI) via 12 mm diameter Teflon (DuPont™) tubing, through a nipple in the room wall, to the mixing box in the magnet room. At the mixing box, the air passes through two 1 l glass odor saturation canisters, one containing 250 ml of a non-odorous solvent and the other containing 250 ml of an odorous solution based on the same solvent. Both odor saturators are placed in a thermal bath held at 37.5°C. Air from both saturators passes through individual flow meters (Ohmeda, Columbia, MD) set at 15 l/min (LPM) each and then through 8 m long, 12 mm diameter Teflon tubing to a switching device 20 cm from the subject's head in the magnet bore. An alternating vacuum source at the switching device evacuates either the odorized or non-odorized air, thus maintaining a constant net flow of 15 LPM of either odorized or non-odorized air that fuses with clean air from the dilution pump before entering a face mask. Two 8 m long vacuum lines originate at a switching valve (Red-Hat, Asco, Florham Park, NJ), which is served by a flowmeter-monitored main vacuum line leading out of the magnet suite. Maintaining all three flowmeters (monitoring odorized air, clean air and vacuum) at 15 LPM permits alternating between odor and no-odor conditions by activating the switching valve on the vacuum line, without any change in final flow rate (15 LPM).

Clean air from the dilution pump (Healthdyne CPAP, Marietta, GA) flows through 10 m long 20 mm diameter Teflon tubing directly to the fusion point before the mask. One-way flow valves are incorporated at all flow junctions in order to assure clear-air purity. Air streams from both pumps enter the mask that is air-tight around the subject's nose. The mask (Fig. 2) is a modified nasal mask (Respronics, Murrysville, PA), internally coated with Teflon and equipped with five one-way flow valves (Dynalon Check Valve, Dynalab, Rochester, NY) permitting up to 30 LPM flow to leave the mask freely, thus maintaining a microenvironment around the subject's nose. Odor-concentration can be estimated and adjusted by changing the flow rate of the dilution pump that is initially set at a maximum of 15 LPM (for estimating concentration using flow parameters see: Dravnieks, 1975; Prah et al., 1995). Stimulus

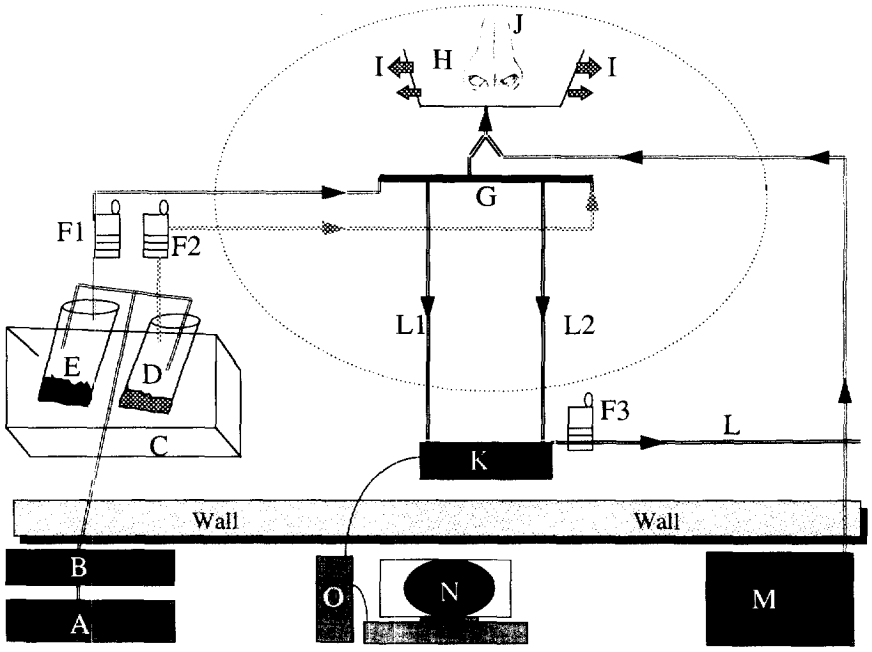

Fig. 1. Diagram of olfactometer. Objects not drawn to scale. Dotted circle represents 5 m radius in which no ferrous components are present. (A) main pump at 50 PSI; (B) activated Charcoal filter; (C) thermal bath at 37.5°C; (D) saturation canister with odor; (E) saturation canister with diluent; (F1) flowmeter for clean air at 15 LPM; (F2) flowmeter for odorized air at 15 LPM; (F3) flowmeter for vacuum at 15 LPM; (G) switching device; (H) nasal mask; (I) one-way flow valves on mask; (J) nose; (K) 24 VDC solenoid; (L1) alternating vacuum of clean air; (L2) alternating vacuum of odorized air; (L) main vacuum line out of magnet suite; (M) dilution pump with internal filter and flow control from 0–15 LPM; (N) microcomputer; and (O) valve interface + 24 V power source. Elements A, B, M, N and O, are all in the control room adjacent to the scanner room, and are connected to their respective targets via nipples in the scanner room wall.

rise and fall times are estimated at less than 500 ms. Estimation is based on final flow rate (15–30 LPM), volume of the mask (60 ml) and the distance between the switching point and the mask (20 cm). When the final flow rate is 15 LPM (main pump 15 LPM, dilution pump 0 LPM, odor concentration = maximum), odor rise and fall time is 480 ms. When final flow rate is 30 LPM (main pump 15 LPM, dilution pump 15 LPM, odor concentration = minimum), odor rise and fall time is 240 ms. Switching from odor to no-odor conditions provides no visual, tactile, auditory, or thermal cues to the subject who is wearing the mask. All elements of the stimulus generator that come in contact with the air-streams are made of either glass or Teflon, thus minimizing the danger of contamination due to odor-adherence in the system.

Fig. 2. Nasal mask. (A) One-way flow valves permitting air to leave the mask; (B) velcro straps; (C) connector to air from switching device; and (D) connector to air from dilution pump.

The apparatus can be modified to accommodate more than one odor in two different configurations. The first configuration offers control over two different odors by duplicating the system and coupling the dual systems at the switching device (Fig. 3A). This configuration maintains the same high temporal resolution for both odor/no-odor and interodor switching. The second multi-odor configuration redirects the odorized air-flow through different odor saturation canisters by way of Teflon-coated switching valve/s (Red-Hat, Asco, Teflon coated) (Fig. 3B). The second configuration allows for the incorporation of numerous different odors, but inter-odor switching time increases from 500 ms to 3 s, because the initial odor must first clear the 8 m long line and mask following each switch.

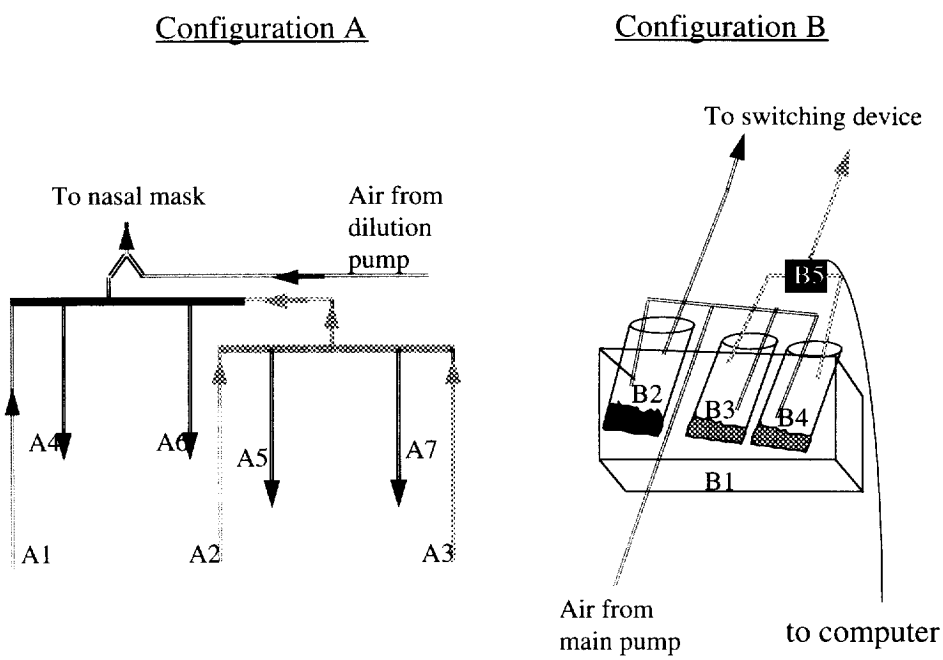

Fig. 3. Multiple odor configurations. Configuration A with rise time of less than 500 ms: (A1) Clean air; (A2) first odor air stream; (A3) second odor air stream; (A4) vacuum, 'on' during odor condition; (A5) vacuum 'on' during second odor condition; (A6) vacuum, 'on' during no-odor condition; and (A7) vacuum, 'on' during first odor condition. Note that a solenoid switches between A4 and A6 for the odor and no-odor alteration and a second solenoid swiches between A5 and A7 for alternating between the two odors. Configuration B with rise time of 3 s: (B1) Thermal bath; (B2) saturation canister with dilutent; (B3) saturation canister with first odorant; (B4) saturation canister with second odorant; and (B5) teflon coated solenoid permitting flow of only one odorant.

2.2. Experimental arrangement—prior to the experiment

In order to eliminate air-flow in the nasal passages during the time when the subject is not supposed to be sniffing, subjects are taught velopharyngeal (soft palate) closure, which is a technique of breathing in and out through the mouth while blocking the passage of air in the nose by obtaining conscious control over the velopharyngeal flap (Kobal, 1981). Such control is obtained in feedback practice sessions using a nasal mask that whistles as long as air is blocked from flowing down the nasal passages. Subjects who can not achieve such control do not participate in the study.

A major obstacle arising from the inherently long duration of an imaging study is the rapid habituation of the olfactory system (for review see: Cometto-muñiz and Cain, 1995). In order to avoid habituation to the point of no response, each subject participates in a pretest equivalent in duration to the intended scan and set to low odor concentration. The subject is cued randomly throughout the pretest for ability to detect the odor and if total habituation has occurred (lack of response to the presence of an odor), odor concentration is increased. This process is repeated until a suprathreshold concentration is reached at which the subject can reliably detect the presence of odor despite the prolonged stimulation.

2.3. Experimental arrangement—during experimentation

Odor stimuli are generated in an alternating block design of odor and no-odor conditions (Fig. 4A). We found the best half-block duration to be 40 s and a minimum of 4 blocks is used summing to a duration of 320 s.

Subjects lie in the scanner with the mask tightly secured to the nose by way of head-encasing Velcro straps. Each subject is fitted with a bite-bar in order to eliminate head-motion. The bite bar is custom molded from dental cement (Kerr, Romulus, MI) to fit the subject's front teeth dental impression, permitting a gap on the sides to enable oral breathing. Using the dominant hand the subject can press one of four buttons, connected via optic cables to a Carnegie Mellon button box (New Micros, Dallas, Texas) that interfaces with a Macintosh Performa computer. This computer is also connected to a video projector (Resonance Technology, Van Nuys, CA) that projects text or images on a screen situated within the scanner bore, viewed by the subject via a mirror.

Experimental design is programmed on the same computer using 'PsyScope' software (Cohen et al., 1993). During a detection task (Fig. 4B), a line of script reading: 'SNIFF AND RESPOND, IS THERE AN ODOR? PRESS THE RIGHT BUTTON FOR YES

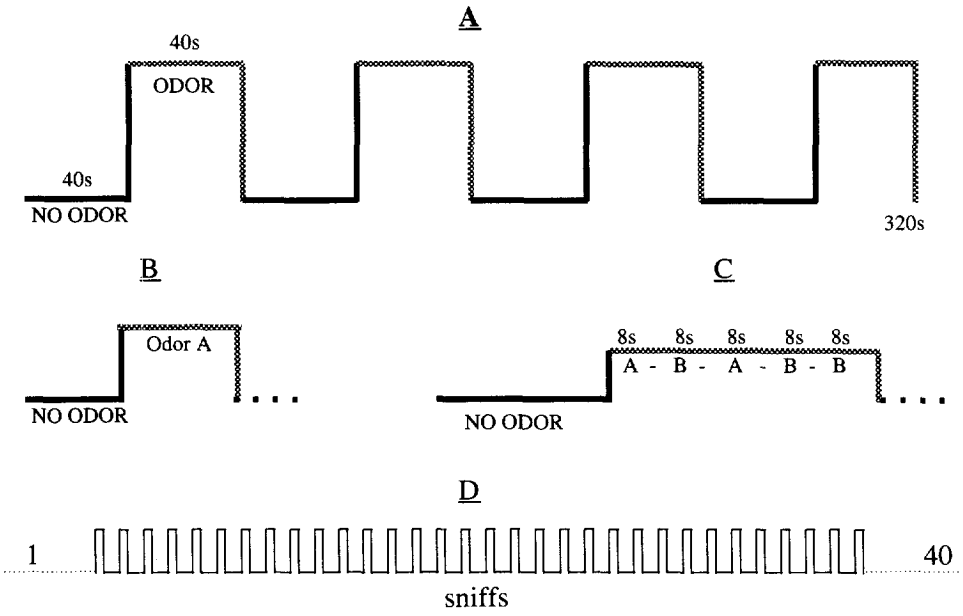

Fig. 4. Experimental design. (A) 40 s half-blocks of odor and no-odor alternate eight times, summing at experiment duration of 320 s; (B) in a detection task, the odor half-block consists of the same odorant throughout the 40 s; (C) in an identification task, different odors are randomly present during the odor half-block (e.g. odor A/odor B); and (D) throughout the entire study, subjects sniff and respond once every 8 s, such that five sniffs are taken in every half-block (40 sniffs within a scan).

OR THE LEFT BUTTON FOR NO' is projected to the subject once every 8 s. The subject sniffs and then responds by using the index finger only to press one of the buttons. In an identification task (Fig. 4C) the projected message reads: 'SNIFF AND RESPOND, WHAT ODOR WAS THAT? PRESS THE RIGHT BUTTON FOR ODOR 'A', MIDDLE BUTTON FOR ODOR 'B', LEFT BUTTON FOR NO-ODOR' (this is equivalent to a multiple choice recognition task; in an actual experiment the letters 'A' and 'B' are substituted with common names of the odorants in use such as 'Vanilla' or 'Crayons' and the subject's familiarity with these odors and names is pre-validated). The number of sniffs and button presses is thus balanced over the odor and the no-odor conditions. Response accuracy and reaction time are recorded on the computer. The same computer is also coupled to the scanner and is used to trigger the scan, thus maintaining synchronization between the task and data acquisition. Sniff duration can be controlled by instructing the subject to maintain the sniff as long as a dot remains projected on the screen. Psychophysical data, however, suggest that optimal olfactory perception is achieved through natural sniffing, which has average duration of 0.4 s (Laing, 1983).

2.4. Imaging parameters

Imaging is performed using a 1.5 T whole-body MRI scanner (General Electric Medical Systems Signa, Rev. 5.5 Echospeed). For functional imaging, two 12.7 cm diameter local receive coils are used for signal reception. Coils are placed with the center of each coil immediately dorsal to the temporal mandibular joint on an imaginary line between the corner of the eye and the ear canal. This location is chosen so as to maximize signal from orbitofrontal and ventromedial temporal regions. A T2* sensitive gradient echo spiral sequence (Noll et al., 1995), which is relatively insensitive to cardiac pulsatility motion artifacts (Glover and Lee, 1995) is employed with parameters of TR = 720 ms, TE = 40 ms, flip angle = 65°. Spatial resolution is set by a 153 × 153 voxel matrix covering a 42 × 42 cm field of view resulting in an in-plane resolution of 2.75 × 2.75 mm. Four interleaves are collected for each frame, with a total acqisition time of 2.88 s per frame. 115 frames are acquired for a total scan duration of 331 s.

Eight 4 mm thick slices with a 2 mm inter-slice gap are acquired at an oblique plane (Fig. 5) traversing from the frontal pole to the temporal pole (typically 30° clockwise to the AC-PC plane). This slice orientation is chosen so as to maximize the volume of olfactory cortex within a single slice. Most regions of interest fall within the third slice, which typically includes a large portion of the orbitofrontal cortices and piriform and entorhinal areas within the ventromedial temporal region. These structures would not be simultaneously covered within a single 4 mm thick slice taken at standard coronal or horizontal planes (Talairach and Tournoux, 1988).

The experimental sequence automatically initiates 12 s following scanning onset, allowing for the first four

frames to be discarded before analysis in order to eliminate any transients arising before the achievement of dynamic equilibrium. T1-weighted flow compensated spin-warp anatomy images (TR = 500 ms, minimum TE) are acquired as a substrate on which to overlay functional data. Structural images of the entire brain are also obtained at the coronal plane (90° to AC-PC plane). Location of specific regions within the oblique slices is later cross-referenced on the coronals using a cross-referencing algorithm so as to validate anatomical localization of regions-of-interest within standardized coordinates (Talairach and Tournoux, 1988).

2.5. Analysis of functional data

Image reconstruction is performed off-line by transferring the raw data to a Sun SparcStation. A gridding algorithm is employed to resample the raw data into a Cartesian matrix prior to processing with 2d FFT. Once individual images are reconstructed, time series of each pixel are obtained and correlation methods that take advantage of periodically oscillating events are used to analyze functional activation (Friston et al., 1994). Since a considerable percentage of artificial signal that might occur over time could be due to events which are random with respect to the timing of the experiment (e.g. pulsatile blood flow, CSF, or brain movement), correlations of the pixel responses to a reference function that represents the timing of the expected activation (based on the timing of stimulus presentation) are employed to remove artifacts (Bandettini et al., 1993; Lee et al., 1995). As described by Friston et al. (1994), the reference function is computed by convolving a square-wave at the task frequency with a data-derived estimate of the hemodynamic response function. The frequency of the square-wave is computed by dividing the number of task cycles by the duration of the experiment, in this case, four cycles/320 s = 0.0125 Hz. Correlations between the reference function and the pixel response time-series are computed and normalized (Friston et al., 1994). In order to construct functional activation maps, pixels that satisfy the criterion of $z > 1.96$ (representing significance of $p < 0.025$, one-tailed) are selected. This map is then processed with a median filter with a spatial width of two, to emphasize spatially coherent patterns of activation. The filter is employed based on the assumption that pixels with spuriously high z values (i.e. false positives due to type I errors) are less likely to occur in clusters than pixels with genuinely high z values. The resulting activation map is overlaid on a T1-weighted structural image. Motion analysis is performed for all subjects using an algorithm based on correlation of the image with a reference image (Friston et al., 1996) and corrected using a correction algorithm described by Woods et al. (1992). The above analysis scheme has proven successful in analyzing data obtained in these experiments. In this manuscript we focus primarily on the method of odor generation. For an additional elegant approach to the analysis of the functional data in the ventral temporal region see Yang et al. (1997).

Fig. 5. Slice orientation traversing from frontal pole to temporal pole, maximizing the volume of regions of interest from the olfactory system within one slice.

3. Example of implementation

3.1. Procedures

A 21 year old healthy right-handed non-smoking female subject participated in the study. The subject signed a document of informed consent and was paid $10 an hour. The subject came to the laboratory one day before scanning to practice velopharyngeal closure with the feedback mechanism described in Section 2.2. The subject was scanned twice during two separate detection tasks as described in section 2.3, once using the odorant Vanillin and once using Propionic acid (v 110-4 and 24 035-4, Aldrich, Milwaukee, WI) both diluted in double-distilled de-ionized water at 20% v/v and 5% v/v in the saturation canisters, respectively. These odorants were chosen because propionic acid, like most odorants, elicits a response

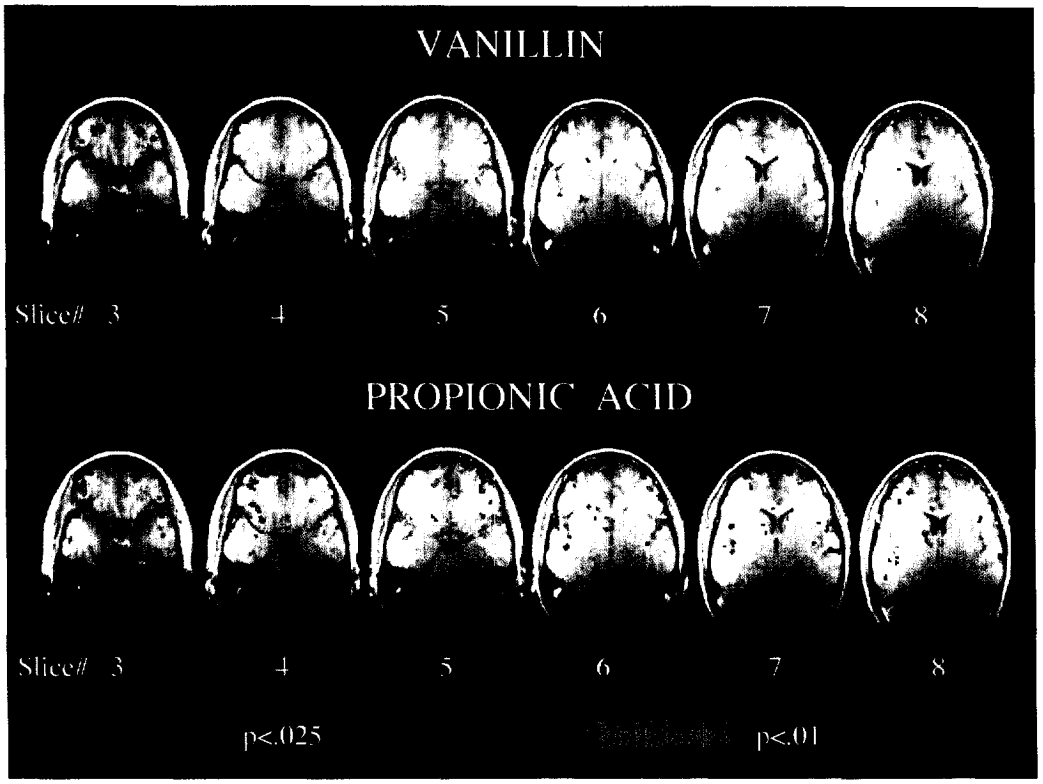

Fig. 6. Activation in the six slices covering regions of interest during detection of vanillin and detection of propionic acid. No significant activation was seen in slices 1 and 2. Pixels in which activity is significantly correlated to the task are color-coded from $z = 1.96$ ($p < 0.025$) to $z = 2.33$ ($p < 0.01$). Vanillin induced significant activation primarily in the cingulate gyrus and orbitofrontal cortices (slice 3), superior frontal (slices 4 and 7), middle frontal (slice 8), and region of the hypothalamus (slice 6). Propionic acid induced significantly greater activation than vanillin in the same regions and in addition, in the superior temporal gyrus (slices 3–8), ventromedial frontal gyrus (slice 5), piriform cortex (slices 4–6), Insula (slices 6 and 7) and thalamus (slice 8).

both in the olfactory nerve (CNV 1) and the trigeminal nerve (CNV 5), whereas vanillin elicits a response in the olfactory nerve alone (Doty et al., 1978). Data were then analyzed according to procedures described in sections 2.4 and 2.5. Following the scan, the subject rated the odorants on a hedonic evaluation scale of 1–10, representing a continuum from very pleasant to very unpleasant, respectively.

3.2. Results

Response accuracy in the detection tasks was 100%. After the scan the subject hedonically rated vanillin at '1' (very pleasant) and propionic acid at '9' (unpleasant). Analysis of motion revealed no significant motion. Vanillin induced significant activation primarily in the cingulate gyrus and orbitofrontal cortices (Fig. 6, slice 3), superior frontal (slices 4 and 7), middle frontal (slice 8) and region of the hypothalamus (slice 6). Propionic acid induced significantly greater activation than vanillin. Additional activation was seen when stimulating with propionic acid, in the superior temporal gyrus (slices 3–8), ventromedial frontal gyrus (slice 5), piriform cortex (slices 4–6), Insula (slices 6 and 7) and thalamus (slice 8).

4. Discussion

Regions of activity seen in both scans of the subject described above are in agreement with lesion and PET findings. Olfactory deficits occur following lesions in medial temporal and inferior frontal areas (Rausch and Serafetinides, 1975; Potter and Butters, 1980; Eslinger et al., 1982; Eskenazi et al., 1983). A PET study (Zatorre et al., 1992) found increased activation following stimulation with odors in the piriform, orbitofrontal, insular and medial frontal cortices and a second PET study (Zald and Pardo, 1997) found increased activation in the orbitofrontal and amygdala. Using MEG, Kettenmann et al. (1996) observed odor-induced activity in the superior temporal lobe. Our method also revealed superior temporal lobe activation (Fig. 6). The additional activations seen in this study and not in the study by Kettenmann, may be due to the difference in the behavior of the subjects. In the present study, subjects were constantly sniffing, whereas in the Kettenmann study subjects did not sniff. The activation in this study is not directly sniff-induced (sniffing was held as a constant baseline throughout the task and sham scans with constant sniffing, but without odor, did not induce

activation), but the sniff may be a necessary **carrier** for the odorant to excite additional cortical regions. The additional regions of activation seen in this study are also in agreement with lesion and PET findings cited above. The convergence of MEG, lesion and PET findings with our results supports the validity of the fMRI method we have described. Furthermore, we have used these methods to obtain consistent and reliable results from eight other subjects who participated in 12 scanning sessions (four of the subjects were tested twice) with two different odorants, totaling 32 scans (Sobel et al., 1996, 1997a,b). Similar patterns of activation were seen in all these scans. Four of these eight subjects also participated in sham scans in which no odor was generated. No activation was seen in the sham scans. The absence of predictable brain activation in the sham validates the integrity of the no-odor condition in precluding ambient odors and of the stimulus generating apparatus in controlling stimulus delivery. Additional support for the integrity of the no-odor condition can be seen in the behavioral performance of eight different subjects performing the task (Table 1). If any part of the system had been contaminated, one would expect subjects to detect an odor during the no-odor condition. Table 1 shows that the number of false alarms was negligible (six out of 160 responses).

In addition to localizing regions involved in olfactory processing, this experimental design enables the comparison of different odor-stimuli. Most odorants induce a combined response from the trigeminal and the olfactory nerves. Doty et al. (1978) however, found two odorants, vanillin and decanoic acid, that elicit a response in the olfactory nerve alone. In the above study, we found that the trigeminal stimulant (propionic acid) induced significantly more activity than the pure olfactory stimulant (vanillin). This effect, which can be seen in Fig. 6, was also seen in eight additional subjects (results to be published in detail elsewhere). This finding is in agreement with Kobal et al. (1992), who found that evoked potentials induced by trigeminal stimuli were easier to produce and larger in amplitude than those induced by a pure olfactant.

Table 1
Behavioral performance of eight subjects using the methods described above

Subject	False alarms	Hits	Accuracy (%)
1	2	19	90
2	0	20	100
3	2	19	90
4	0	20	100
5	0	19	97.5
6	0	20	100
7	0	20	100
8	2	19	90

Subject's performance indicates that the system reliably switched between odor and no-odor conditions, and that no odor was perceived in the no-odor condition. In each scan the subject is cued to respond 40 times, of which 20 are in the no-odor phase. There were only six false alarms over the 160 responses obtained in the no-odor phase. Mean accuracy was 96%.

The increased activation induced by propionic acid may be the result of either the recruitment of a second pathway (the trigeminal), or an increase in activation within the olfactory pathway due to the negative hedonic value and increased intensity associated with propionic acid relative to vanillin. This question can be addressed by comparing activation following stimulation with olfactory and trigeminal stimuli which have been matched for odor intensity and hedonic value. Activation induced by stimulation with odors may also represent the cumulative effect of additional systems excited by the odorant, such as gustatory activation, or stimulation of nerves such as the terminal, vagal, glossopharyngeal and vomeronasal (VNO). The olfactometer cannot limit the stimulation to any of these intranasal nerves. However, these possibilities may be addressed by using the methods we have described to stimulate with various air-borne stimuli that are known to excite these systems in varying degrees, thus isolating the separate components. The methods described above may be used in addressing these and other topics in olfactory processing.

Acknowledgements

This work was supported by grants AG12995, MH30854, P41RR09784 from the Phil and Allen trust. We thank H. Bahlman, J. Wine and R. Fernald for their generous help with equipment and C. Vaidya for modeling the mask.

References

Bandettini PA, Wong EC, Hinks RS, Tikofsky JS, Hyde JS. Time course EPI of human brain function during task activation. Magn. Reson. Med. 1992;25:390–7.

Bandettini PA, Jesmanowicz A, Wong EC, Hyde JS. Processing strategies for time-course data sets in functional MRI of the human brain. Magn. Reson. Med. 1995;30:161–73.

Cohen JD, MacWhinney B, Flatt M, Provost J. PsyScope: A new graphic interactive environment for designing psychology experiments. Behav. Res. Methods Inst. Comp. 1993;25:257–71.

Cometto-muñiz, JE, Cain, WS, Olfactory adaption. In: Doty RL, editor. Handbook of Olfaction and Gustation. New York: Marcel Dekker, 1995:257–282.

Desmond JE, Sum JM, Wagner AD, Demb JB, Shear PK, Glover GH, Gabrieli JDE, Morell MJ. Functional MRI measurement of language lateralization in Wada-tested patients. Brain 1995;118:1411–9.

Doty RL, Brugger WE, Jurs PC, Orndorff MA, Snyder PJ, Lowry LD. Intranasal trigeminal stimulation from odorous volatiles: Psychometric responses from anosmic and normal humans. Physiol. Behav. 1978;20:175–85.

Doty, RL, Kobal, G. Current trends in the measurement of olfactory function. In: Doty, RL, editor. Handbook of Olfaction and Gustation. New York: Marcel Dekker, 1995:191–226.

Dravnieks, A. Instrumental aspects of olfactometry, In: Moulton, ATDG, Johnston, JW, editors. Methods in Olfactory Research. New York: Academic Press, 1975:1–62.

Eskenazi B, Cain WS, Novelly RA, Friend KB. Olfactory functioning in temporal lobectomy patients. Neuropsychol. 1983;21:365–74.

Eslinger PJ, Damasio AR, Van Hoesen GW. Olfactory dysfunction in man: anatomical and behavioral aspects. Brain Cog. 1982;1:259–85.

Friston KJ, Jezzard P, Turner R. Analysis of functional MRI time-series. Hum. Brain Mapp. 1994;1:153–71.

Friston KJ, Williams SR, Howard R, Frackowiak RSJ, Turner, R. Movement-related effects in fMRI time-series. Magnet. Res. Med. 1996;35:346-355

Gabrieli JDE, Desmond JE, Demb JB, Wagner AD, Stone MV, Vaidya CJ, Glover GH. Functional magnetic resonance imaging of semantic memory processes in the frontal lobes. Psychon. Sci. 1996;7:278–83.

Glover GH, Lee AT. Motion artifacts in fMRI: Comparison of 2DFT with PR and spiral scan methods. Magn. Reson. Med. 1995;33:624–35.

Kettenmann B, Jousmaki V, Portin K, Samlelin R, Kobal G, Hari R. Odorants activate the human superior temporal sulcus. Neurosci. Lett. 1996;203:143–5.

Kettenmann, B, Grodd, W, Erb, M, Pfister, M, Klusmann, A, Hulsmann, M, Klose, U, Kobal, G. Cortical olfactory areas identified by fMRI. AChemS XIX, 1997 (abstract).

Kobal, G. Elektrophysiologische Untersuchungen des Menschlichen Geruchssinnes. Stuttgart: Thieme, 1981.

Kobal, G. Pain-related electrical potentials of the human nasal mucosa elicited by chemical stimulation. Pain, 1985:151–163.

Kobal G, Hummel T, Van Toller S. Differences in human chemosensory evoked potentials to olfactory and somatosensory chemical stimuli presented to left and right nostrils. Chem. Senses 1992;17:233–44.

Kobal, G, Hummel, T. Olfactory evoked potentials in humans. In: Getchell LMBTV, Doty RL, Snow, JB, editors. Smell and Taste in Health and Disease. New York: Raven Press, 1991:255–275.

Koizuka I, Yano H, Nagahara M, Mochizuki R, Seo R, Shimada K, Kubo T, Nogawa T. Functional imaging of the human olfactory cortex by magnetic resonance imaging and its related specialities. J. Oto-Rhino-Laryngol. 1994;56:273–5.

Laing DG. Natural sniffing gives optimum odor perception for humans. Perception 1983;12:99–117.

Lee AT, Glover GH, Meyer CH. Discrimination of large venous vessels in time-course spiral blood-oxygen-level-dependent magnetic-resonance functional neuroimaging. Magn. Reson. Med. 1995;33:745–54.

Noll DC, Cohen JD, Meyer CH, Schneider W. Spiral k-space MRI of cortical activation. J. Magn. Reson. Imaging 1995;5:49–56.

Posner MI, Petersen SE, Fox PT, Raichle ME. Localization of cognitive operations in the human brain. Science 1988;240:1627–31.

Potter H, Butters N. An assessment of olfactory deficits in patients with damage to prefrontal cortex. Neuropsychology 1980;18:621–8.

Prah JD, Sears SB, Walker JC. Modern approaches to air dilution olfactometry. In: Doty RL, editor. Handbook of Olfaction and Gustation. New York: Marcel Dekker, 1995:227–256.

Rausch R, Serafetinides EA. Specific alterations of olfactory function in humans with temporal lobe lesions. Nature 1975;255:557–8.

Sobel N, Prabhakaran V, Desmond J, Glover G, Sullivan E, Gabrieli J. A method for generating olfactory stimuli for fMRI. Society for Neuroscience 26th Annual Meeting Abstract:106.8, 1996.

Sobel N, Prabhakaran V, Desmond J, Glover G, Sullivan E, Gabrieli JDE. Sniff-driven activation in the piriform cortex of humans. Abstract in AChemS XIX, 1997 (abstract).

Sobel N, Prabhakaran V, Desmond J, Glover G, Sullivan E, Gabrieli J. Sniffing and Smelling: Separate subsystems in human olfactory cortex, 1997.

Talairach J, Tournoux P. Co-planar Stereotaxic Atlas of the Human Brain. Stuttgart: Thieme, 1988.

Woods RP, Cherry SR, Mazziotta JC. A rapid automated algorithm for accurately aligning and re-slicing positron emission tomography images. J. Comput. Assist. Tomogr. 1992;16:620–33.

Yang QX, Dardzinski BJ, Li S, Eslinger PJ, Smith MB. Multi-Gradient Echo with Susceptibility Inhomogeneity Compensation (MGESIC): Demonstration of fMRI in olfactory cortex at 3.0 T. Magn. Reson. Med. 1997;37:331–5.

Zald DH, Pardo JV. Emotion, olfaction and the human amygdala: Amygdala activation during aversive olfactory stimulation. Proc. Natl. Acad. Sci. USA 1997;94:4119–24.

Yousem D, Williams S, Simmons A, Doty R, Kroger H. Functional magnetic resonance imaging using olfactory stimulants. AChemS XIX, 1997 (abstract).

Zatorre RJ, Jones-Gotman M, Evans AC, Meyer E. Functional localization and lateralization of human olfactory cortex. Nature 1992;360:339–41.